An Analysis of the Effect of Lower Extremity Strength on Impact Severity During a Backward Fall

Reuben Sandler

Stephen Robinovitch

Biomechanics Laboratory,
Department of Orthopaedic Surgery,
San Francisco General Hospital and
University of California, San Francisco,
San Francisco, CA 94110

At least 280,000 hip fractures occur annually in the U.S., at an estimated cost of $9 billion. While over 90 percent of these are caused by falls, only about 2 percent of all falls result in hip fracture. Evidence suggests that the most important determinants of hip fracture risk during a fall are the body's impact velocity and configuration. Accordingly, protective responses for reducing impact velocity, and the likelihood for direct impact to the hip, strongly influence fracture risk. One method for reducing the body's impact velocity and kinetic energy during a fall is to absorb energy in the lower extremity muscles during descent, as occurs during sitting and squatting. In the present study, we employed a series of inverted pendulum models to determine: (a) the theoretical effect of this mechanism on impact severity during a backward fall, and (b) the effect on impact severity of age-related declines (or exercise-induced enhancements) in lower extremity strength. Compared to the case of a fall with zero energy absorption in the lower extremity joints, best-case falls (which involved 81 percent activation of ankle and hip muscles, but only 23 percent activation of knees muscles) involved 79 percent attenuation (from 352 J to 74 J) in the body's vertical kinetic energy at impact (KE_v), and 48 percent attenuation (from 3.22 to 1.68 m/s) in the downward velocity of the pelvis at impact (v_v). Among the mechanisms responsible for this were: (1) eccentric contraction of lower extremity muscles during descent, which resulted in up to 150 J of energy absorption; (2) impact with the trunk in an upright configuration, which reduced the change in potential energy associated with the fall by 100 J; and (3) knee extension during the final stage of descent, which "transferred" up to 90 J of impact energy into horizontal (as opposed to vertical) kinetic energy. Declines in joint strength reduced the effectiveness of mechanisms (1) and (3), and thereby increased impact severity. However, even with reductions of 80 percent in available torques, KE_v was attenuated by 50 percent. This indicates the importance of both technique and strength in reducing impact severity. These results provide motivation for attempts to reduce elderly individuals' risk for fall-related injury through the combination of instruction in safe falling techniques and exercises that enhance lower extremity strength. [DOI: 10.1115/1.1408940]

Keywords: Falls, Hip Fracture, Strength, Mathematical Modeling, Biomechanics

Introduction

Among elderly individuals living in the United States, falls are the number one cause of nonfatal injury, and number two cause of injury-related death [1]. They account for approximately 90 percent of hip and wrist fractures in this age group [2,3], and nearly 40 percent of traumatic vertebral fractures [4]. The annual medical costs in the U.S. associated with hip fractures alone is approximately $8.9 billion [5].

While one's risk for fall-related fracture is influenced by bone density and fall frequency, growing epidemiological evidence suggests that it depends most strongly on the mechanics of the fall. This makes sense from a biomechanical perspective, given that the energy and force capable of being generated during a fall from standing height substantially exceed values required to fracture the proximal femur or distal radius [6–10].

The most important determinant of injury risk during a fall is impact location. Direct impact between the hip and the ground increases elderly individuals' risk for hip fracture by approximately 30-fold [11–13]. Impacting the outstretched hand reduces hip fracture risk by about threefold and increases risk for wrist fracture by approximately 20-fold [11]. Fall direction influences impact configuration and injury risk, with sideways falls creating the highest risk for hip fracture, and backward falls creating the highest risk for wrist and vertebral fracture [4,11,14].

Biomechanical considerations suggest that injury risk also associates with impact velocity. For example, our previous ''pelvis-release'' experiments [15,16] indicate that, while body mass and soft tissue thickness have important influences, impact velocity is by far the strongest determinant of femoral impact force during a fall on the hip. While it has been impossible to include this variable directly in epidemiological studies of fracture risk, previous studies have shown associations between hip fracture and both fall height [2,12] and body height [17], presumably due to the effect of these variables on impact velocity.

Finally, declines in lower extremity strength substantially increase hip fracture risk in the event of a fall [13,18–20]. While the mechanism underlying this association is unknown, some authors have suggested that it relates to one's ability to absorb energy in the lower extremity muscles during the descent phase of the fall, and thereby reduce the kinetic energy and velocity of the body at impact [21]. Consideration of acts such as sitting and squatting indicate the potential effectiveness of this mechanism. When a typical adult descends from standing to sitting, the total potential energy of the body decreases by approximately 200 J. However, due to energy absorption in the lower extremity muscles during descent, the body's downward velocity and kinetic energy at the instant of chair contact tend to be minimal [22]. Previous biome-

Contributed by the Bioengineering Division for publication in the JOURNAL OF BIOMECHANICAL ENGINEERING. Manuscript received by the Bioengineering Division July 2, 1999; revised manuscript received May 16, 2001. Associate Editor: M. G. Pandy.

chanical studies suggest that young subjects utilize this mechanism to reduce impact severity during falling, since observed contact velocities are well below those predicted by simple mathematical models of free fall [22–25]. However, little is known regarding the falling techniques that minimize impact severity, and how the efficacy of these depends on lower extremity strength.

Accordingly, the main goal of the present study was to examine the theoretical effect on fall severity of lower extremity muscle contractions during descent. A related goal was to determine how one's ability to reduce impact severity is affected by age-related declines (or exercise-induced enhancements) in lower extremity strength. Given the complex out-of-plane motions typically associated with sideways falls [23–25], we restricted our efforts in this preliminary study to two-dimensional models of backward falls. For this particular class of falls, our research questions were: (1) What attenuations in impact velocity and kinetic energy can theoretically be attained by the development of lower extremity joint torques during descent? (2) What is the theoretical effect on impact velocity and kinetic energy of declines in available joint torques?

Methods

The energy absorbed by a given joint during the descent phase of falling depends on the magnitude of joint torque and the magnitude of joint rotation. To determine how each of these variables theoretically affects impact severity, we developed one-link, two-link, and three-link inverted pendulum models of backward falls from standing height (Fig. 1). Among the assumptions inherent in these models were: (1) that movement is restricted to the sagittal plane, (2) that the feet remain stationary and in contact with the ground throughout descent, and (3) that contraction of muscles spanning the ankles, knees, or hips generates a net joint torque, which can instantly change in magnitude and direction. The one-link model simulates a fall where the knees and hips remain extended throughout descent, while rotation and energy absorption occur at the ankles. The two-link model simulates a fall where the knees are maintained in extension, while rotation and energy absorption occur at the ankles and hips. The three-link model simulates a fall where rotation and energy absorption occur at the ankles, knees, and hips. In each model, the lengths, masses, and moments of inertia of the various links were representative of an adult female of height 1.6 m and body mass 53.7 kg [26].

Each model incorporated ideal torque generators to simulate the net effect of bilateral (equal right and left side) contraction of muscles spanning the ankles, knees, and hips. The effect of joint strength (or degree of muscle activation) on impact severity was determined by conducting simulations with different ''strength factors'' applied to each joint, ranging from zero to 100 percent of peak attainable values measured in young healthy females under isometric conditions (Table 1). For a given joint, the same strength factor was applied to flexor and extensor torques. However, in the two-link and three-link models, the strength factor of one joint was varied independently of that applied to the other joint(s). For example, a three-link model simulation with strength factors of 75 percent at the ankles, 25 percent at the knees, and 50 percent at the hips would involve 150 Nm of ankle plantarflexor torque, 68 Nm of ankle dorsiflexor torque, 88 Nm of knee extensor torque, 39 Nm of knee flexor torque, 125 Nm of hip extensor torque, and 65 Nm of hip flexor torque.

Based on experimental evidence of joint torque-rotation behavior during sits and self-initiated backward falls [22], the direction of joint torque always acted to raise (or retard downward motion of) the center of gravity of the link directly above the joint (Figs. 1 and 2). Consequently, in the two-link and three-link models, a reversal in the inclination of the trunk from forward to behind the vertical caused hip torque to change instantly from extensor to flexor, and vice versa. Similarly, in the three-link model, a reversal in the inclination of the shin from forward to behind the vertical caused ankle torque to switch abruptly from plantarflexor to dorsiflexor, and vice versa. It should be noted that, in real life, changes in the magnitude and/or direction of joint torques are gradual rather than instantaneous, due to finite rates of motor neuron recruitment and de-recruitment, and finite rates of change in muscle tension following neural activation.

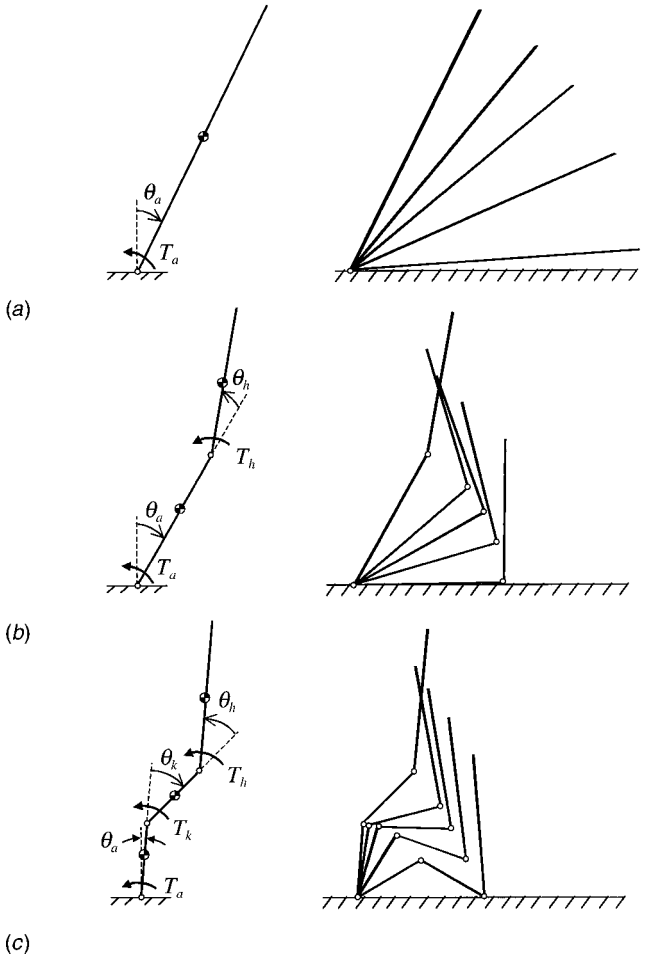

Fig. 1 Typical descent kinematics associated with: (*a*) one-link model, (*b*) two-link model, and (*c*) three-link model (T_a=ankle torque; T_k=knee torque; T_h=hip torque; θ_a=ankle rotation; θ_k=knee rotation, θ_h=hip rotation).

Each model was ''released'' from a configuration where the whole-body center-of-gravity was posterior to the ankle joint, and the total gravitational potential energy of the body (with respect to the ankles) equaled 410 J. Accordingly, the one-link model descended from an initial configuration involving 27 deg of plantar-

Table 1 Maximum joint torques in model simulations

Joint	Torque Direction	Maximum Torque* (Nm)	Reference
Ankle	Dorsiflexor	90	Sepic, *et al.*, 1986
	Plantarflexor	200	Sepic, *et al.*, 1986
Knee	Flexor	155	Murray, *et al.*, 1985
	Extensor	350	Murray, *et al.*, 1985
Hip	Flexor	130	Cahalan, *et al.*, 1989
	Extensor	250	Cahalan, *et al.*, 1989

*Sum of that acting at the right and left joint.

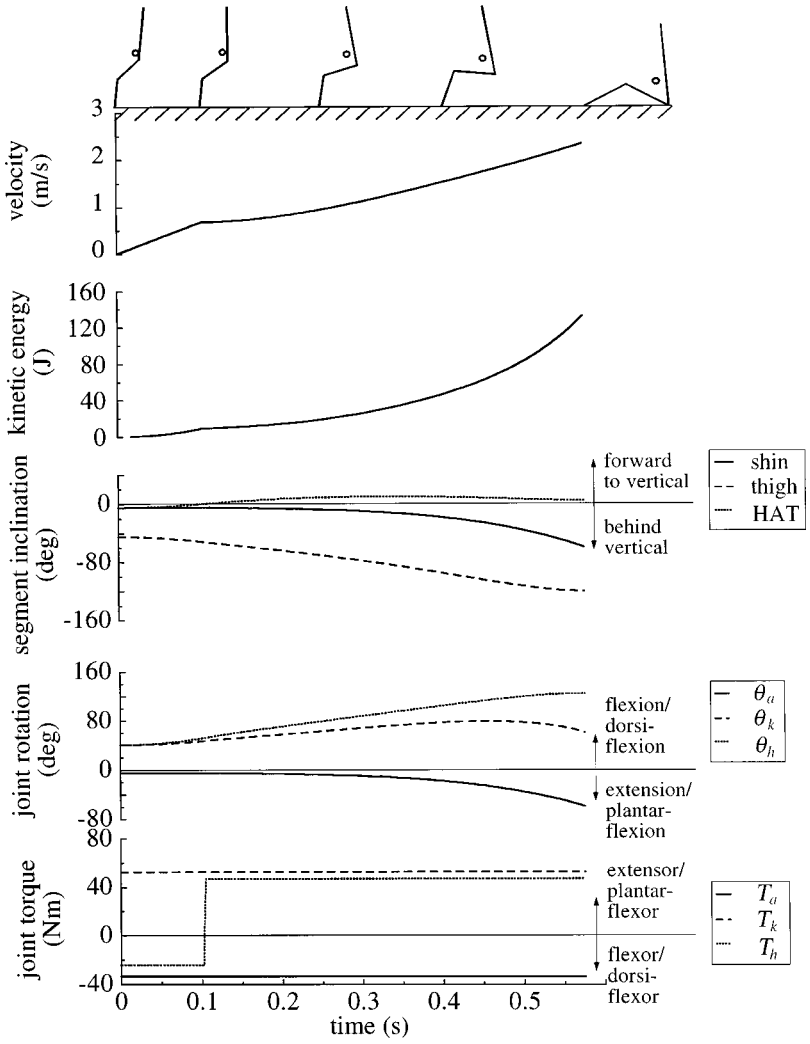

Fig. 2 Typical temporal variations in the vertical (downward) velocity of the pelvis, vertical kinetic energy of the body, link inclinations (with respect to the vertical), joint rotations, and joint torques during a simulated fall with the three link model. Ankle torque is dorsiflexor and eccentric throughout descent. Knee torque is extensor and eccentric until the final stage of descent. Hip torque is initially flexor and concentric, but switches to extensor (and eccentric) when the trunk moves forward to the vertical. This is accompanied by abrupt declines in the slopes of the downward velocity and kinetic energy traces.

flexion at the ankles (Fig. 1). The two-link model descended from a configuration involving 30 deg of plantarflexion and 20 deg of hip flexion. The three-link model descended from a configuration involving 5 deg of plantarflexion, 40 deg of knee flexion, and 40 deg of hip flexion. In all simulations, initial angular velocities were set to zero. These initial conditions were selected to roughly describe those involved in a series of tether-release (falling) experiments conducted recently in our laboratory (currently unpublished). They are not necessarily intended to reflect typical body configurations after real-life slips or trips.

MATLAB was used to numerically integrate the equations of motion (see Appendix A). At each integration step, the analysis routine computed translational and angular velocities of each link, and corresponding magnitudes of whole-body kinetic energy (see Appendix B). Modifications to MATLAB's ordinary differential equation solver were made to accommodate reversals in the direction of joint torque during a given simulation.

Each simulation proceeded until the occurrence of impact, signified by the vertical position of the pelvis descending below the ankles. The change in potential energy (ΔPE) during descent was defined as $\Delta PE = PE_i - PE_f$, where i and f represent initial and final states. Our previous studies indicate that during an unexpected backward fall, individuals maintain the knees and hips moderately flexed during descent, and impact the ground with the trunk in a near-upright configuration [23]. Therefore, to focus our attention on realistic falling scenarios and alleviate the need to incorporate joint ''stops'' into the model, we disregarded simulations involving initial impact to the knees or head, or the occurrence of hyperflexion or hyperextension at the knees or hips.

The work performed at a given joint was determined by numerically integrating the area under the torque-rotation curve. Joint work was defined positive if the direction of torque was opposite to the direction of joint rotation (i.e., eccentric). Checks were made to ensure that conservation of energy was maintained throughout all simulations, as defined by $\Delta PE = KE_{\text{tot}} + W_{\text{tot}}$, where W_{tot} is the sum of joint work, and KE_{tot} is the total (translational+rotational) kinetic energy of the body at the instant of pelvis impact.

Impact severity was represented by the vertical component of the body's total kinetic energy (KE_v) and the vertical (downward)

Table 2 Results of simulations with the one-link model, as a function of ankle strength*

Parameter	Available Strength Factor §				
	100	70	40	20	0
Ankle torque ¶	100	70	40	20	0
Total joint work W_{tot} (J)	98.8	69.2	39.5	19.8	0.0
Total kinetic energy KE_{tot} (J)	311.2	340.9	370.5	390.2	410.0
Rotational kinetic energy KE_{rot} (J)	43.9	48.1	52.2	54.9	57.7
Vertical kinetic energy KE_v (J)	267.3	292.8	318.3	335.3	352.3
% attenuation †	24	17	10	5	-
Vertical pelvis velocity v_v (m/s)	2.80	2.93	3.05	3.13	3.22
% attenuation †	13	9	5	3	-

* For all one-link simulations, ΔPE = 410 J and KE_h = 0.

§ Maximum available dorsiflexor torque, as a percentage of value shown in Table 1.

¶ Dorsiflexor torque (as a percentage of that shown in Table 1) yielding lowest magnitude of KE_v.

† Relative to value with zero ankle torque.

velocity of the pelvis (v_v) at the instant of pelvis contact (Appendix B). Descent of the one link model with zero ankle torque served as a "worst-case fall" source of comparison. Under these conditions, KE_v = 352 J and v_v = 3.22 m/s (Table 2). The effect on impact severity of global declines in lower extremity strength was determined by comparing best-case falls involving strength factors no greater than 20 (simulating 80 reduction in strength), 40, 70, and 100 percent (no impairment). For simplicity, "best-case" falls were those that minimized KE_v. Attention was also focused on impact severity during simulations with the two-link and three-link models involving zero ankle torque, which simulated falls from a narrow base of support.

Table 3 Results of best-case simulations with the two-link model, as a function of overall joint strength

Parameter	Available Strength Factor §				
	100(A)	100(B)*	70	40	20
Ankle torque ¶	100	0	70	32.5	20
Hip torque ¶	22.5	32.5	27.5	30	20
Potential energy change ΔPE (J)	305.7	305.2	306.4	304.4	312.8
% decrease†	25	26	25	26	24
Total joint work W_{tot} (J)	140.9	64.7	115.9	89.2	75.8
Total kinetic energy KE_{tot} (J)	165.9	241.8	191.8	216.6	237.8
Rotational kinetic energy KE_{rot} (J)	13.4	22.7	17.0	20.4	9.1
Horizontal kinetic energy KE_h (J)	19.1	33.4	24.6	30.2	8.8
Vertical kinetic energy KE_v (J)	133.4	185.7	150.2	166	219.9
% attenuation †	62	47	57	53	38
Vertical pelvis velocity v_v (m/s)	2.53	2.94	2.56	2.77	3.43
% attenuation †	21	9	20	14	-7

§ Maximum available joint torques, as a percentage of values shown in Table 1.

* $\%T_a^{max} = 0$ throughout descent.

¶ Joint torque (as a percentage of that shown in Table 1) yielding lowest magnitude of KE_v.

† Relative to value occurring in one-link model simulation with zero ankle torque.

Table 4 Results of best-case simulations with the three-link model, as a function of overall joint strength

Parameter	Available Strength Factor §				
	100(A)	100(B)*	70	40	20
Ankle torque ¶	81.25	0	68.75	37.5	18.75
Knee torque ¶	22.5	7.5	17.5	15	10
Hip torque ¶	81.25	56.25	68.75	18.75	18.75
Potential energy change ΔPE (J)	292.1	286.9	292.2	291.1	282.9
% decrease†	29	30	29	29	31
Total joint work W_{tot} (J)	133.4	87.8	109.0	105.1	86.1
Total kinetic energy KE_{tot} (J)	169.0	203.1	190.6	186.3	196.9
Rotational kinetic energy KE_{rot} (J)	4.1	5.4	3.4	1.7	6.6
Horizontal kinetic energy KE_h (J)	91.3	36.9	79.9	52.1	12.7
Vertical kinetic energy KE_v (J)	73.6	160.8	107.3	132.5	177.6
% attenuation †	79	54	70	62	50
Vertical pelvis velocity v_v (m/s)	1.68	2.69	2.03	2.33	2.81
% attenuation †	48	16	37	28	13

§ Maximum available joint torques, as a percentage of values shown in Table 1.

* $\%T_a^{max} = 0$ throughout descent.

¶ Joint torque (as a percentage of that shown in Table 1) yielding lowest magnitude of KE_v.

† Relative to value occurring in one-link model simulation with zero ankle torque.

Results

Impact severity was reduced substantially by the generation of lower extremity joint torques during descent. The best-case fall with the one link model, which involved a strength factor of 100 percent at the ankles, resulted in attenuations of 24 percent in KE_v and 13 percent in v_v (Table 2). The best-case fall with the two-link model, which involved strength factors of 100 percent at the ankles and 23 percent at the hips, resulted in attenuations of 62 percent in KE_v and 21 percent in v_v (Table 3). The best-case fall with the three-link model, which involved strength factors of 81 percent at the ankles, 23 percent at the knees, and 81 percent at the hips, resulted in attenuations of 79 percent in KE_v and 48 percent in v_v (Table 4).

Comparison of outcome parameters from the three models indicates that rotation (and torque generation) at each joint influenced fall severity (Fig. 4). For example, comparison of best-case falls with the one and two link models suggests that rotation and torque generation at the hips reduces KE_v by up to 50 percent (from 267 to 133 J) and v_v by up to 10 percent (from 2.80 to 2.53 m/s). This is due to two phenomena. First, by generating eccentric extensor torque at the hips during descent, W_{tot} increased from 99 to 141 J. Second, by flexing the hips to impact the ground with the trunk in a near-upright configuration, ΔPE decreased from 410 to 306 J. Comparison of best-case falls with the two and three-link models suggests that rotation and torque generation at the knees can attenuate KE_v by a further 44 percent (from 133 to 74 J), and v_v by a further 34 percent (from 2.53 to 1.68 m/s). Rather than being due to differences in W_{tot}, ΔPE, or KE_{tot}, this arose mainly from knee extension during the final stage of descent, which allowed for a "transferring" of energy from the vertical to horizontal direction, and a corresponding increase from 19 to 91 J in the horizontal kinetic energy of the body at impact (KE_h). Finally, comparing best-case simulations with the three-link model involving zero and 100 percent available strength factors at the ankles indicates that ankle torque can increase W_{tot} and KE_h by up to 34 and 60 percent, respectively, and decrease KE_v and v_v

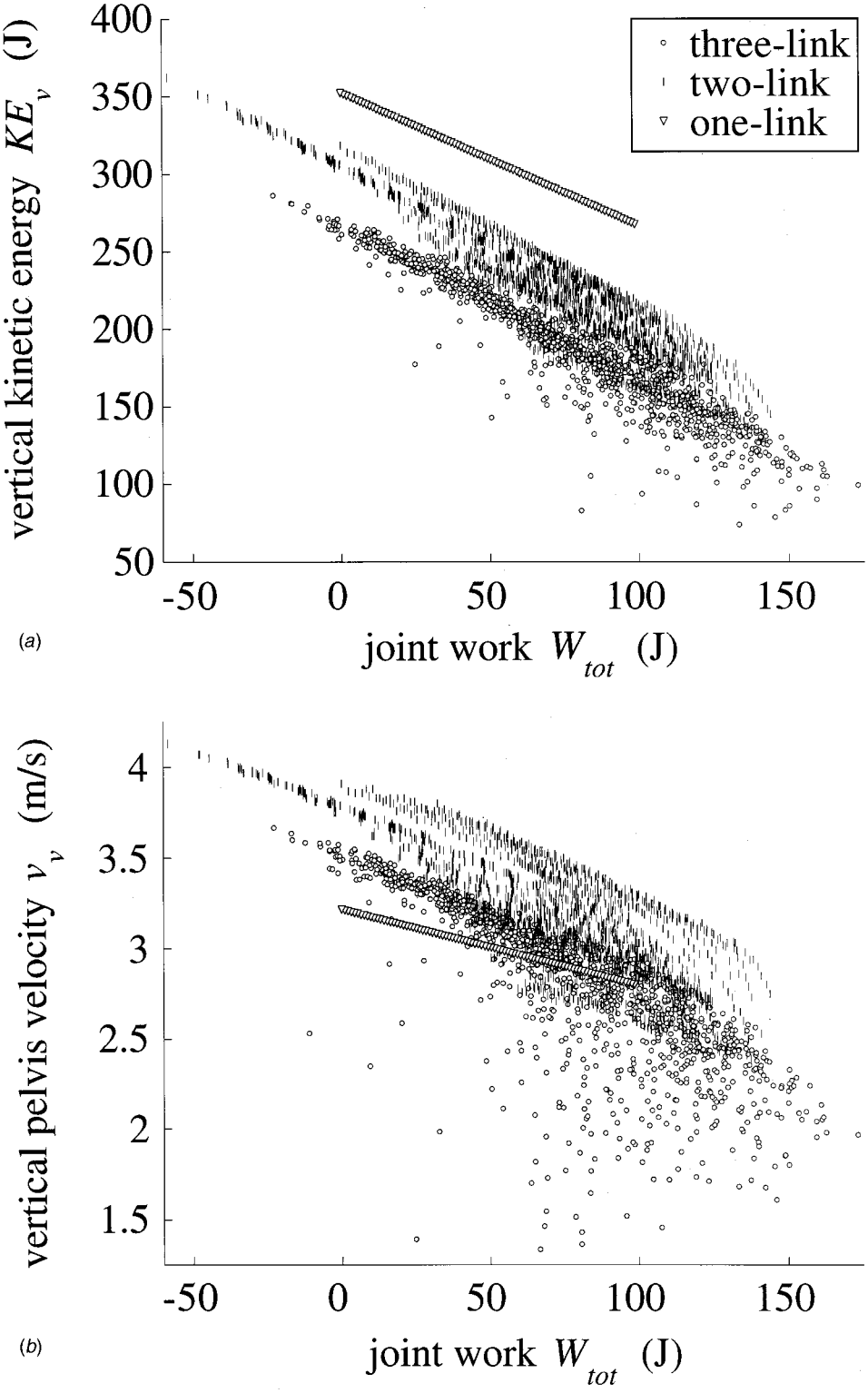

Fig. 3 Association between total joint work (W_{tot}) and (*a*) vertical kinetic energy (KE_v) at the instant of impact and (*b*) pelvis velocity (v_v) at the instant of impact. For each of the three models, W_{tot} associated with KE_v and v_v (see text for correlation statistics). However, variations in KE_h and knee flexion at impact caused considerable scatter in these relations for the three-link model.

by up to 119 and 60 percent. This explains why particularly severe falls may occur from a narrow base of support (e.g., a stair, a ladder step, or the edge of a curb).

Impact severity increased with global reductions in joint strength (Fig. 4). This occurred for two reasons. First, in simulations with the three-link model, declines in available strength factors led to a reduction in KE_h, and an increase in the percent of total impact energy that was manifest as vertical as opposed to

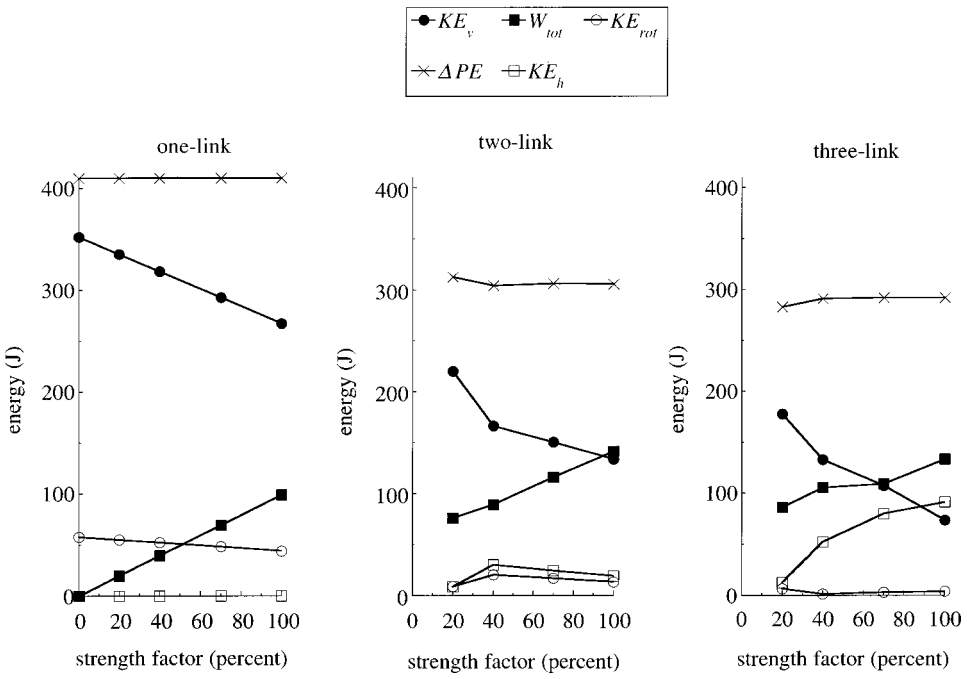

Fig. 4 Effect of available strength factors on total joint work during descent (W_{tot}), change in potential energy during descent (ΔPE), vertical kinetic energy at impact (KE_v), horizontal kinetic energy at impact (KE_h), and rotational kinetic energy at impact (KE_{rot}). Conservation of energy dictates that $\Delta PE = W_{tot} + KE_v + KE_h + KE_{rot}$. Declines in available strength factors cause an increase in KE_v, by reducing W_{tot} and (for the three-link model) decreasing KE_h. When compared to the one link model, ΔPE and KE_v values are lower in simulations with the two-link and three-link models. This is due to hip flexion and impact of the trunk in a nearly vertical orientation.

horizontal kinetic energy. Second (and more importantly), for each model, declines in available strength factors led to a reduction in W_{tot}: A 1 percent decline in available strength caused an average decrease of approximately 0.8 J in W_{tot} (Fig. 4 and Tables 2, 3, and 4). In turn, W_{tot} associated negatively with both KE_v and v_v, with a 10 J decrease in W_{tot} causing an average increase of approximately 10 J in KE_v and 0.09 m/s in v_v (Fig. 3). Coefficients of determination (R^2 values) for the association between v_v and W_{tot} (Fig. 3(*a*)) were 1.0 for the one-link model, 0.69 for the two-link model, and 0.65 for the three-link model (in all cases, $p<0.001$). R^2 values for the association between KE_v and W_{tot} (Fig. 3(*b*)) were 1.0 for the one-link model, 0.88 for the two-link model, and 0.92 for the three-link model (again, $p<0.001$ in all cases).

However, when compared to our worst-case fall, substantial reductions in impact severity were observed even with large declines in joint strength. For example, with strength factors of 19 percent at the ankles, 10 percent at the knees, and 19 percent at the hips, the three-link model yielded $KE_v = 178$ J and $v_v = 2.81$ m/s, attenuations of 50 and 13 percent, respectively (Table 4). Several mechanisms were responsible for this. First, even when accompanied by relatively small magnitudes of joint torque, large joint rotations allowed for nonnegligible magnitudes of W_{tot}. Second, simulations with the two-link and three-link models continued to involve impact with the trunk in a nearly upright configuration, and a corresponding large reduction in ΔPE. Finally, optimal strength factors at the hip in the two link model and knee in the three link model were always no greater than 30 percent, and were therefore affected little by simulated declines in strength.

Discussion

Our results indicate that substantial reductions in fall severity can be achieved through the development of lower extremity joint torques during descent. For example, when compared to our worst-case fall, best-case falls with the three-link model resulted in attenuations of 79 percent in KE_v and 48 percent in v_v. Among the mechanisms responsible for this were: (1) the generation of eccentric (braking) torques in the lower extremity joints during descent, which resulted in up to 150 J of energy absorption; (2) the occurrence of impact to the ground with the trunk in an upright configuration, which reduced the change in potential energy during descent by 100 J; and (3) the occurrence of knee extension during the final stage of descent, which transferred up to 90 J of impact energy from the vertical to horizontal direction.

Our results also suggest that one's ability to land safely depends at least as much on "technique" as it does on strength. For example, reductions of up to 50 percent in KE_h were observed even with simulated declines of 80 percent in peak joint torques. Thus, properly executed "relaxed" falls should involve considerably lower risk for injury than rigid falls involving minimal knee and hip flexion (which might arise from fear or limitations on joint flexibility).

Further evidence for the importance of technique in safe landing is the observation that best-case falls with the two-link and three-link models did not involve maximum torque activation. For example, best-case falls with the two link model involved relatively small magnitudes of hip torque (strength factors of approximately 20 percent); larger values caused the trunk to impact in an inclined position, which increased ΔPE and decreased W_{tot}. Best-case falls with the three-link model involved large hip torques but small knee torques (strength factors of approximately 20 percent), which facilitated large knee and hip flexions and thus large W_{tot}.

Competing biomechanical phenomena influenced the effect of joint rotation on impact severity. Knee and hip flexion tended to reduce KE_v by increasing W_{tot} and decreasing ΔPE. However, their effect on v_v was more complex. On the one hand, such flexions caused the body's center-of-gravity to move closer to the

ankles. This reduced the body's ''effective'' moment of inertia and, due to conservation of angular momentum, increased its effective rotational velocity (with respect to the ankles). This accounts for the relatively large magnitudes of v_v predicted by the two-link model. On the other hand, knee flexion reduced the distance between the pelvis and ankles, and therefore the magnitude of v_v for a given rotational velocity. This explains why v_v was relatively small in best-case falls with the three-link model.

Our simulations complement experimental evidence regarding the effect on fall severity of energy absorption in the lower extremity during descent. In a recent experimental study of backward falls with young subjects, we found that hip impact velocities averaged 1.45 ± 0.5 (S.D.) m/s and vertical kinetic energies at impact averaged 31.6 ± 24 J [22]. These values are lower than our current predictions, probably due to the fact that our models descended from an initial configuration of imbalance, while subjects in the experimental study self-initiated their descent from a stable standing position, and absorbed a substantial amount of energy in their lower extremity joints before reaching a state of imbalance. In an earlier study [23], we found that, in addition to absorbing energy during descent, the responses elicited during unexpected falls serve to arrange the body in a safe landing configuration. For example, subjects tended to avoid impact to the head and pelvis by impacting the ground with the outstretched hands (and in the case of forward or sideways falls, the knees), and by rotating of the trunk about an inferior–superior axis (during sideways falls). However, backward falls in that study involved qualitatively similar joint rotations to those observed here, and while pelvis impact velocities were higher (averaging 2.55 ± 0.85 m/s), they were again well below values predicted by free fall assumptions.

Data also suggest that impact severity during sideways falls may be reduced by the generation of flexion rotations and eccentric extensor torques at the knees and hips during descent. The strongest evidence of this comes from van den Kroonenberg and co-workers' [23–25] study of body movements during self-initiated sideways falls. Their reported hip impact velocities averaged 2.75 ± 0.42 (S.D.) m/s, and their estimates of kinetic energy at impact averaged 188 J, or 71 percent lower than subjects' potential energy during standing. They also found that, when subjects were instructed to ''fall as relaxed as they could'' as opposed to ''naturally,'' reductions occurred in average values of trunk angle at impact (14 deg versus 22 deg from the vertical) and hip impact velocity (2.66 m/s versus 2.86 m/s). One factor apparently contributing to the latter observation was greater knee flexion during descent, and a subsequent reduction in the distance between the pelvis and ankles (which, as observed in our three link model simulations, reduces the translational velocity of the pelvis for a given rotational velocity).

Several limitations exist to this study. We examined only a single torque activation strategy (i.e., attempting to raise the link above the joint), and while preliminary experimental results suggest this to be realistic [22], alternative and potentially more effective muscle activation strategies may exist. We also neglected cases involving hyperextension or hyperflexion at the knees or hips, which might be examined through realistic simulation of joint stops. Moreover, we simulated the net effect of muscle contractions about a joint with ideal torque actuators, and did not account for the effect on torque development of variables such as the intactness of proprioceptive and vestibular signals, the state of potentiation and firing frequency of motor neurons, the intrinsic (force-length and force-velocity) properties of muscle and in-series connective tissue, the anatomical arrangement of muscles spanning each joint, and the degree of co-contraction of agonist and antagonist muscles. We doubt that adding these features to the model would substantially change our conclusions regarding the effect on impact severity of available torque magnitudes. However, it would provide a more robust tool for systematically examining how fall severity is influenced by specific neuromuscular pathologies.

We also assumed that the feet remain fixed on the ground and that dorsiflexor (or plantarflexor) moments can be generated at the ankles throughout descent. During an actual fall, the toes or even both feet may rise off the ground. Falls involving complete loss of foot–ground contact (due, for example, to a violent slip or trip) would likely be severe, since it is ultimately the development of vertical foot reaction forces that decelerates the body's downward movement.

The fact that we did not restrict plantarflexion rotation probably caused us to overestimate energy absorption at the ankle in simulations with the one link and two link models, where the ankle rotated to an unrealistic 90 deg of plantarflexion before impact. However, it probably had a small effect on the realism of simulations with the three link model, since experimental studies suggest that eccentric dorsiflexor torques are developed throughout the final stage of descent during a backward fall, despite the tendency for the toes to rise off the ground before pelvis impact [22].

We did not include simulation results describing the effect of body size or body mass distribution on impact severity. However, preliminary analyses indicate that (although impact severity indices scale with body height and weight) relatively large and unrealistic changes in the body mass distribution are required to invalidate our current conclusions.

Finally, we considered two indices of impact severity (KE_v and v_v), based on the notion that these govern impact force and fracture risk [9,16]. However, we acknowledge that greater understanding is required of the variables that best reflect injury risk during a fall. Impacting the ground with the trunk horizontal increases the change in potential energy of the fall, but offers the potential advantage of increasing the contact area available for energy absorption. However, we are cautious about recommending this falling technique, due to the risk it may create for head impact. Our decision to consider only vertical (as opposed to horizontal or rotational) kinetic energy as injurious may be debated. However, we believe this is justified for the following reasons: (1) the observation that in all simulations, KE_{rot} values were small compared to KE_v, (2) the expectation that substantial magnitudes of KE_h can be absorbed through deformation of soft tissue layers (skin, fat, and muscle) without the transmission of large forces to the underlying bone, and (3) the fact that our conclusions would be affected little by considering KE_{tot} as our index of impact severity, instead of KE_v.

It is difficult to determine accurately the difference in injury risk associated with our best and worst-case fall simulations. However, for the case of hip fracture, this can be estimated by considering a backward fall that results in impact to the lateral aspect of the hip, as opposed to the buttocks (due, for example, to axial rotation during the final stage of descent). Let us assume that the range of contact velocities and impact energies associated with our current simulations apply to such falls. We have previously found that, during a fall on the lateral aspect of the hip, approximately 34 J of impact energy is absorbed in the soft tissues overlying the proximal femur [27]. In our worst-case fall, this leaves 318 J of energy to be absorbed in the proximal femur and pelvis, which greatly exceeds the energy required to fracture the elderly cadaveric proximal femur (measured by Lotz et al. [28] to average 21.5 ± 13.5 (S.D.) J). However, in our best-case fall, only 40 J of energy must be absorbed through bone deformation, and thus fracture risk should be considerably lower. A comparison of predicted contact forces yields similar conclusions. Our previous studies suggest that, during impact to the lateral aspect of the hip, the body behaves essentially like a mass-spring system, having an effective mass m of approximately 0.5*body mass, and an effective spring stiffness k of approximately 43 kN/m [16]. The peak contact force applied to the hip will be $\sqrt{mk}v_v$, or (for our 53.7 kg female) 3460 N in our worst-case fall and 1805 N in our best-case fall. The former is well within the range of force found

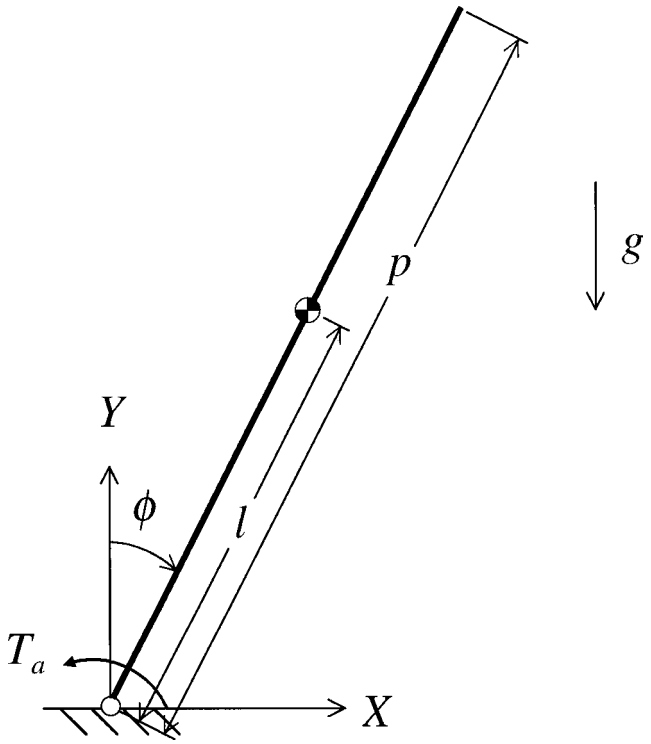

Fig. 5 One-link inverted pendulum model. See Appendix A for definition of variables.

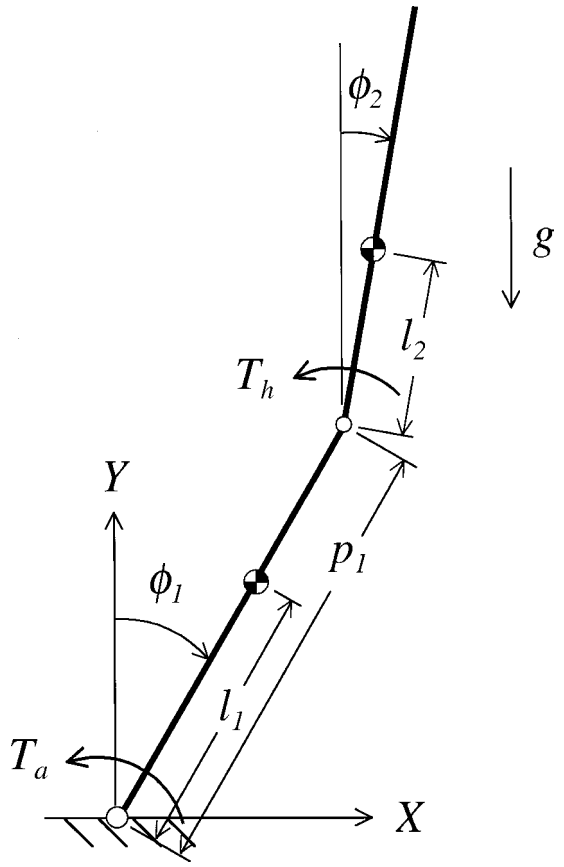

Fig. 6 Two-link inverted pendulum model. See Appendix A for definition of variables.

to fracture the elderly cadaveric femur (measured by Courtney et al. [29] to average 4170±1590 (S.D.) N), while the latter is considerably below it.

These results justify efforts to enhance safe landing abilities, particularly among elderly individuals who are at high risk for falls. Our current data suggest that such programs should incorporate exercises that enhance lower extremity strength and flexibility in the sagittal plane, and instruction in safe landing techniques, such as bending the knees and maintaining the trunk upright during descent. Further research is required to understand better the biomechanical and neuromuscular variables that govern impact severity during forward and sideways falls. Given that hip fractures are by far the most important fall-related injury, such research should focus particularly on techniques (such as axial rotation of the trunk and use of the outstretched hands to break the fall [23]) that enhance elderly individuals' ability to avoid direct impact to the hip during sideways falls.

Acknowledgments

This work was supported by a Biomedical Engineering Research Grant from the Whitaker Foundation, a grant from the Centers for Disease Control (R49/CCR019335), a grant from the National Institutes of Health (RO1AR46890), and a grant from the Academic Senate of the University of California. The authors wish to thank Qi Liu, M.S., Jeff Cortez, M.S., and Liz Hsiao, M.S. for their assistance in developing the models used in the present study.

Appendix A

Equations of Motion. The equations of motion for our inverted pendulum models were derived using Lagrange's equation:

$$\frac{d}{dt}\left(\frac{\partial L}{\partial \dot{\phi}_i}\right)-\frac{\partial L}{\partial \phi_i}=Q_i$$

where $L\equiv T-V$, T is the total kinetic energy of the system, V is the total potential energy of the system, Q_i are the generalized forces, ϕ_i are the degrees of freedom, and $i=1,2,\ldots n$.

One-Link Model. The potential energy of the one link model (Fig. 5) is

$$V=mgl\cos\phi$$

where m is the mass of the entire link, l is the distance between the ankle joint and the link center of gravity, ϕ is the angle between the link and the vertical, and g is the gravitational constant, 9.81 m/s^2. Note from comparing Fig. 5 and Fig. 1 that $\phi=\theta_a$. The kinetic energy is

$$T=\frac{1}{2}I^0\dot{\phi}^2$$

where $I^0=mr^2$ is the mass moment of inertia of the link about the ankle, and r is the radius of gyration (provided by [26] for given magnitudes of body height and body weight).

Applying Lagrange's equation results in the following nonlinear equation of motion:

$$I^0\ddot{\phi}-mgl\sin\phi=-T_a$$

where T_a is torque at the ankles, positive in the counterclockwise direction.

Two-Link Model. The total potential energy of the two link model (Fig. 6) is

$$V=m_1l_1g\cos\phi_1+m_2g(p_1\cos\phi_1+l_2\cos\phi_2)$$

where the subscripts 1 and 2 represent the lower and upper links, respectively, m_i are the link masses, l_i are the distances from the

joints to the link centers of gravity, p_1 is the length of the lower link, and ϕ_i are the angles between the links and the vertical. Note from comparing Fig. 6 and Fig. 1 that $\phi_1=\theta_a$ and $\phi_2=\theta_a-\theta_h$.

The total kinetic energy of two-link model is

$$T=\frac{1}{2}(I_1^0+m_2p_1^2)\dot{\phi}_1^2+\frac{1}{2}(I_2^{cg}+m_2l_2^2)\dot{\phi}_2^2 + m_2p_1l_2\dot{\phi}_1\dot{\phi}_2\cos(\phi_1-\phi_2),$$

where $I_1^0=m_1r_1^2$ is the moment of inertia of the bottom link about the ankles, r_1 is the radius of gyration of the bottom link about the ankles, $I_2^{cg}=m_2r_2^2$ is the moment of inertia of the top link about its center of gravity, and r_2 is the radius of gyration of the top link about its center of gravity. Again, magnitudes of r_i are provided by [26].

Lagrange's equation yields the following coupled nonlinear equations of motion:

$$(I_1^0+m_2p_1^2)\ddot{\phi}_1+(m_2p_1l_2\cos(\phi_1-\phi_2))\ddot{\phi}_2 + (m_2p_1l_2\sin(\phi_1-\phi_2))\dot{\phi}_2^2-(m_1l_1+m_2p_1)g\sin\phi_1 = T_h-T_a$$

and

$$(I_2^{cg}+m_2l_2^2)\ddot{\phi}_2+(m_2p_1l_2\cos(\phi_1-\phi_2))\ddot{\phi}_1 -(m_2p_1l_2\sin(\phi_1-\phi_2))\dot{\phi}_1^2-m_2l_2g\sin\phi_2=-T_h,$$

where T_a and T_h are torques at the ankles and hips respectively, positive in the counterclockwise direction.

Three-Link Model. Due to the complexity of the energy expression and equations of motion for the three-link model, these are not provided here. Angeles [30] provides a complete derivation and presentation of these equations (although we noted five typesetting errors, which the author has informed us are now corrected in an errata).

Appendix B

Definition of Vertical Kinetic Energy. The kinetic energy of a system of links can be defined as:

$$KE_{\text{tot}}=\sum_{i=1}^{n}\left[\frac{1}{2}m_iv_i^2+\frac{1}{2}I_i\dot{\theta}_i^2\right],$$

where n is the number of links, v_i is the translational velocity of the ith link's center of gravity, $\dot{\theta}_i$ is the rotational velocity of the ith link, m_i is the mass of the ith link, $I_i=m_i\rho_i^2$ is the mass moment of inertia of the ith link, and ρ_i is the radius of gyration of the ith link about its center of gravity.

An alternate form of KE_{tot} separates the translational velocity into vertical and horizontal components:

$$KE_{\text{tot}}=\sum_{i=1}^{n}\left[\frac{1}{2}m_iv_{hi}^2+\frac{1}{2}m_iv_{vi}^2+\frac{1}{2}I_i\dot{\theta}_i^2\right],$$

or

$$KE_{\text{tot}}=\sum_{i=1}^{n}\left[KE_{hi}+KE_{vi}+KE_{\text{roti}}\right],$$

where the subscripts h, v, and rot represent horizontal, vertical, and rotational, respectively. Removing the summation notation gives $KE_{\text{tot}}=KE_h+KE_v+KE_{\text{rot}}$, which is the format utilized in the present manuscript.

References

[1] United States Department of Health and Human Services, Public Health Service, 1993. *Healthy People 2000: National Health Promotion and Disease Prevention Objectives*. Washington, DC.

[2] Grisso, J. A., Kelsey, J. L., Strom, B. L., Chiu, G. Y., Maislin, G., O'Brien, L. A., Hoffman, S., and Kaplan, F., 1991, "Risk Factors for Falls as a Cause of Hip Fracture in Women. The Northeast Hip Fracture Study Group," N. Engl. J. Med., **324**, pp. 1326–1331.

[3] Spaite, D. W., Criss, E. A., Valenzuela, T. D., Meislin, H. W., and Ross, J., 1990, "Geriatric Injury: An Analysis of Prehospital Demographics, Mechanisms, and Patterns," Ann. Emerg. Med. , **19**, pp. 1418–1421.

[4] Cooper, C., Atkinson, E. J., Kotowicz, M., O'Fallon, W. M., and Melton, L. J. D., 1992, "Secular Trends in the Incidence of Postmenopausal Vertebral Fractures," Calcif. Tissue Int., **51**, pp. 100–104.

[5] Praemar, A., Furner, S., and Rice, D. P., 1992, "Costs of Musculoskeletal Conditions," in: *Musculoskeletal Conditions on the United States*, American Academy of Orthopaedic Surgeons, Park Ridge, IL, pp. 143–170.

[6] Chiu, J., and Robinovitch, S. N., 1998, "Prediction of Upper Extremity Impact Forces During Falls on the Outstretched Hand," J. Biomech., **31**, pp. 1169–76.

[7] Myers, E. R., Sebeny, E. A., Hecker, A. T., Corocan, T. A., Hipp, J. A., Greenspan, S. L., and Hayes, W. C., 1991, "Correlations Between Photon Absorption Properties and Failure Load of the Distal Radius *in Vitro*," Calcif. Tissue Int., **49**, pp. 292–297.

[8] Spadaro, J. A., Werner, F. W., Brenner, R. A., Fortino, M. D., Fay, L. A., and Edwards, W. T., 1994, "Cortical and Trabecular Bone Contribute Strength to the Osteopenic Distal Radius," J. Orthop. Res., **12**, pp. 211–218.

[9] Courtney, A. C., Wachtel, E. F., Myers, E. R., and Hayes, W. C., 1995, "Age-Related Reductions in the Strength of the Femur Tested in a Fall-Loading Configuration," J. Bone Jt. Surg., Am. Vol., **77A**, pp. 387–395.

[10] Cummings, S. R., and Nevitt, M. C., 1994, "Non-skeletal Determinants of Fractures: The Potential Importance of the Mechanics of Falls. Study of Osteoporotic Fractures Research Group," Osteoporosis Int., **4**, Suppl. 1, pp. 67–70.

[11] Nevitt, M. C., and Cummings, S. R., 1993, "Type of Fall and Risk of Hip and Wrist Fractures: The Study of Osteoporotic Fractures," J. Am. Geriatr. Soc., **41**, pp. 1226–1234.

[12] Hayes, W. C., Myers, E. R., Morris, J. N., Gerhart, T. N., Yett, H. S., and Lipsitz, L. A., 1993, "Impact Near the Hip Dominates Fracture Risk in Elderly Nursing Home Residents Who Fall," Calcif. Tissue Int., **52**, pp. 192–198.

[13] Schwartz, A. V., Kelsey, J. L., Sidney, S., and Grisso, J. A., 1998, "Characteristics of Falls and Risk of Hip Fracture in Elderly Men," Osteoporosis Int., **8**, pp. 240–246.

[14] Greenspan, S. L., Myers, E. R., Kiel, D. P., Parker, R. A., Hayes, W. C., and Resnick, N. M., 1998, "Fall Direction, Bone Mineral Density, and Function: Risk Factors for Hip Fracture in Frail Nursing Home Elderly," Am. J. Med., **104**, pp. 539–545.

[15] Robinovitch, S. N., Hayes, W. C., and McMahon, T. A., 1991, "Prediction of Femoral Impact Forces in Falls on the Hip," ASME J. Biomech. Eng., **113**, pp. 366–374.

[16] Robinovitch, S. N., Hayes, W. C., and McMahon, T. A., 1997, "Distribution of Contact Force During Falls on the Hip," Ann. Biomed. Eng., **25**, pp. 499–508.

[17] Hemenway, D., Feskanich, D., and Colditz, G. A., 1995, "Body Height and Hip Fracture: A Cohort Study of 90,000 Women," Int. J. Epidemiol., **24**, pp. 783–786.

[18] Lord, S. R. W., Williams, P., and Anstey, K. J., 1994, "Physiological Factors Associated With Falls in Older Community Dwelling Women," J. Am. Geriatr. Soc., **42**, pp. 1110–1117.

[19] Nevitt, M. C., Cummings, S. R., Kidd, S., and Black, D., 1989, "Risk Factors for Recurrent Nonsyncopal Falls: A Prospective Study," J. Am. Med. Assoc., **261**, pp. 2663–2668.

[20] Tinetti, M. E., Doucette, J., Claus, E., and Marottoli, R., 1995, "Risk Factors for Serious Injury During Falls by Older Persons in the Community," J. Am. Geriatr. Soc., **43**, pp. 1214–1221.

[21] Cummings, S. R., and Nevitt, M. C., 1989, "A Hypothesis: The Cause of Hip Fractures," J. Gerontol., **44**, pp. 107–111.

[22] Robinovitch, S. N., Chiu, J., Sandler, R., and Liu, Q., 2000, "Impact Severity in Self-Initiated Sits and Falls Associates With Center-of-Gravity Excursion During Descent," J. Biomech., **33**, pp. 863–870.

[23] Hsiao, E. T., and Robinovitch, S. N., 1998, "Common Protective Movements Govern Unexpected Falls From Standing Height," J. Biomech., **31**, pp. 1–9.

[24] van den Kroonenberg, A. J., Hayes, W. C., and McMahon, T. A., 1996, "Hip Impact Velocities and Body Configurations for Voluntary Falls From Standing Height," J. Biomech., **29**, pp. 807–11.

[25] van den Kroonenberg, A. J., Hayes, W. C., and McMahon, T. A., 1995, "Dynamic Models for Sideways Falls From Standing Height," ASME J. Biomech. Eng., **117**, pp. 309–318.

[26] Winter, D. A., 1990, *Biomechanics and Motor Control of Human Movement*, Wiley, New York.

[27] Robinovitch, S. N., McMahon, T. A., and Hayes, W. C., 1996, "Force Attenuation and Energy Absorption by Soft Tissues During Falls on the Hip," J. Orthop. Res., **13**, pp. 956–962.

[28] Lotz, J. C., and Hayes, W. C., 1990, "The Use of Quantitative Computed Tomography to Estimate Risk of Fracture of the Hip From Falls," J. Bone Jt. Surg., Am. Vol., **72A**, pp. 689–700.

[29] Courtney, A. C., Wachtel, E. F., Myers, E. R., and Hayes, W. C., 1994, "Effects of Loading Rate on Strength of the Proximal Femur," Calcif. Tissue Int., **55**, pp. 53–58.

[30] Angeles, J., 1997, *Fundamentals of Robotic Mechanical Systems: Theory, Methods, and Algorithms*, Springer, New York.